Available online at www.sciencedirect.com

ScienceDirect

Nuclear Physics A 982 (2019) 247–250

www.elsevier.com/locate/nuclphysa

XXVIIth International Conference on Ultrarelativistic Nucleus-Nucleus Collisions (Quark Matter 2018)

Study of coherent J/ψ production in lead-lead collisions at $\sqrt{s_{\rm NN}} = 5$ TeV with the LHCb experiment

A. Bursche on behalf of the LHCb collaboration

albert.bursche@cern.ch

Abstract

Coherent production of J/ψ mesons is studied in lead-lead collision data at a nucleon-nucleon centre-of-mass energy of 5 TeV collected by the LHCb experiment. The data set corresponds to an integrated luminosity of about 10 μb^{-1}. The J/ψ mesons are reconstructed in the dimuon final state, where the muons are detected within the pseudorapidity region $2.0 < \eta < 4.5$. The J/ψ mesons are required to have transverse momentum $p_{\rm T} < 1$ GeV and rapidity $2.0 < y < 4.5$. The cross-section within this fiducial region is measured to be $\sigma = 5.3 \pm 0.2$ (stat) $\pm$ 0.5 (syst) $\pm$ 0.7 (lumi) mb. The differential cross-section is also measured in five bins of J/ψ rapidity. The results are compared to predictions from phenomenological models.

Keywords: ultraperipheral collisions, ion collisions, J/ψ production

1. Introduction

In ultra-relativistic heavy-nuclei collisions at the LHC, two-photon and photonuclear interactions are enhanced with respect to strong interactions in ultraperipheral collisions (UPC) when the impact parameters of the two nuclei are larger than the sum of their radii. The collisions are either coherent, where the photon couples coherently to all nucleons, or incoherent, where the photon couples to a single nucleon.

In the case of coherent J/ψ production in UPC, PbPb $\rightarrow$ Pb + J/ψ + Pb, the photon-lead interaction can be modelled by the exchange of two gluons, identified as a single object called a pomeron [1, 2, 3, 4, 5]. This interaction is expected to probe the nuclear gluon-distribution at hard scales of about $m^2_{J/\psi}/4$, where $m_{J/\psi}$ is the J/ψ mass [6, 7].

2. Candidate selection

In this analysis, $J/\psi \rightarrow \mu^+\mu^-$ candidates are selected by the trigger system, requiring at least one muon with a transverse momentum $p_{\rm T} > 900$ MeV, [1] at the hardware level, and the invariant mass of the two

[1] In this note natural units where $c = 1$ are used.

https://doi.org/10.1016/j.nuclphysa.2018.10.069
0375-9474/

muons to be greater than 2.7 GeV, at the software level. In the offline selection, candidates are identified by requiring both muons to have $p_T > 500$ MeV within the pseudorapidity region $2.0 < \eta < 4.5$ and the dimuon invariant mass to be within 65 MeV of the known J/ψ mass pole [8]. In addition, only J/ψ candidates with reconstructed $p_T < 1$ GeV, $2.0 < y < 4.5$ and that form a good-quality vertex are used. Additional activity from the same vertex is vetoed.

3. Cross-section measurement

The cross-section of coherent J/ψ production per unit rapidity is defined within a J/ψ rapidity interval Δy as

$$\frac{d\sigma(\mathrm{PbPb} \to \mathrm{Pb} + J/\psi + \mathrm{Pb})}{dy} = \frac{n_{\mathrm{coh}}}{\varepsilon_y \cdot \Delta y \cdot \mathcal{L} \cdot \mathcal{B}} \tag{1}$$

where ε_y is the total efficiency in each rapidity bin, n_{coh} is signal yield, Δy is the rapidity bin width, $\mathcal{L}$ is the integrated luminosity and $\mathcal{B}$ is the branching fraction $\mathcal{B}(J/\psi \to \mu^+\mu^-) = (5.961 \pm 0.033)\%$ [8].

The integrated luminosity of the data set, $\mathcal{L}$, is determined to be $10.1 \pm 1.3\ \mu\mathrm{b}^{-1}$ [9].

3.1. Signal yield determination

The signal yield, n_{coh}, is determined in two steps. First, a fit to the dimuon invariant mass spectrum is performed to obtain the number of J/ψ candidates, which includes coherent and incoherent J/ψ, and $\psi(2S)$ feed-down components. A fit to the J/ψ transverse momentum, p_T, is used to estimate the number of signal candidates where the nonresonant UPC background is constrained from the first fit.

The number of J/ψ mesons is estimated by fitting the invariant dimuon mass distribution to signal and background components. The J/ψ and $\psi(2S)$ invariant mass distributions are modelled by double-sided Crystal Ball functions, and the nonresonant background by an exponential multiplied by a first-order polynomial. The $\psi(2S)$ parameters, aside from the mean, are constrained in the fit to follow those of the J/ψ. Figure 1 shows the fitted dimuon mass spectrum.

Two resonant background sources are considered: incoherent production of J/ψ and feed-down of photoproduction of $\psi(2S)$ mesons. In order to determine the signal yield in the presence of these backgrounds, a maximum likelihood fit to the natural logarithm of the J/ψ transverse momentum squared, $\log(p_T^2)$ is performed. In this fit, the background and signal are modelled by templates taken from the STARlight event generator [2]. An ad-hoc track momentum smearing is used in order to obtain a similar momentum resolution to the one described in Ref. [10]. The feed-down background is assumed to have the same $\log(p_T^2)$ distribution as the incoherent background. Fig. 1 shows the fit to the $\log(p_T^2)$ distribution.

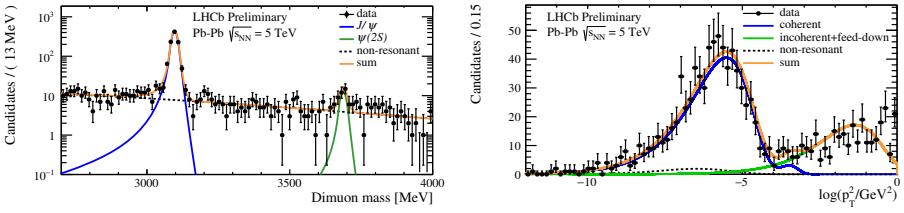

Fig. 1. Distribution of $\log(p_T^2)$ and invariant mass of dimuon candidates after all requirements have been applied. The orange line represents the fit to the data points; the blue line shows the coherent contribution and the green (black) line shows the incoherent and feed-down (nonresonant) component. A fit is performed to data using three different templates obtained from the STARlight event generator. The contribution of (solid blue line) J/ψ, (solid green line) $\psi(2S)$ and (black dashed line) nonresonant dimuons are shown individually and the sum of all contributions is represented by the orange curve.

Table 1. Relative systematic uncertainties considered for the cross-section measurement of coherent J/ψ production. The first two contributions are taken from Ref. [11].

Source	Relative uncertainty (%)
Reconstruction efficiency	2.1–4.5
Selection efficiency	3.2
Hardware trigger efficiency	3.0
Software trigger efficiency	1.6–5.3
Momentum smearing	3.3
Mass fit model	3.9
Feed-down background	5.8
Branching Fraction	0.6
Luminosity	13.0

3.2. Systematic uncertainties

Systematic uncertainties in the measured cross-section are related to the determination of the muon reconstruction and selection efficiencies, the trigger efficiency, the muon momentum smearing, the mass fit signal model and the modelling of the feed-down background. They are described below and summarised in table 1. The largest uncertainty comes from the integrated luminosity determination due to the unusual collision system and the extrapolation method employed.

4. Results

The cross-section for coherent J/ψ production within the fiducial region is calculated using Eq. 1 without the normalisation to the bin width and found to be $\sigma = 5.3 \pm 0.2\,(\text{stat}) \pm 0.5\,(\text{syst}) \pm 0.7\,(\text{lumi})\,\text{mb}$, where the first uncertainty is statistical and the second is systematic and the third is due to the uncertainty on the luminosity. The fiducial region is defined as J/ψ mesons decaying to dimuon final states, where the muons are detected within the pseudorapidity region $2.0 < \eta < 4.5$ and the J/ψ meson is required to have $p_{\text{T}} < 1\,\text{GeV}$ and $2.0 < y < 4.5$. The coherent differential J/ψ production cross-section, measured in bins of J/ψ rapidity, is given in [12]. A comparison of the measurement with theoretical predictions discussed below is shown in Fig. 2.

In the models of Gonçalves et al. [4, 13], Cepila et al. [14] and Mäntysaari et al. [15] the cross-sections are calculated within the framework of the Colour-Dipole model. All of these models describe the data within the uncertainties of that method arising from the need for an assumption for the J/ψ wave function. Assuming the GLC wave function, the prediction with subnucleonic fluctuations [14] is favoured by the LHCb data with respect to the prediction without subnucleonic fluctuations [14]. The model provided by Guzey et al. [1] is based on a perturbative QCD (pQCD) calculation at leading order within the leading-log approximation. The measurement can be described by all used prescriptions for the nuclear structure.

Acknowledgements

The contact author acknowledges support from the European Research Council (ERC) through the project EXPLORINGMATTER, founded by the ERC through a ERC-Consolidator-Grant, GA 647390.

References

[1] V. Guzey, E. Kryshen, M. Zhalov, Coherent photoproduction of vector mesons in ultraperipheral heavy ion collisions: Update for run 2 at the CERN Large Hadron Collider, Phys. Rev. C93 (5) (2016) 055206. arXiv:1602.01456, doi:10.1103/PhysRevC.93.055206.

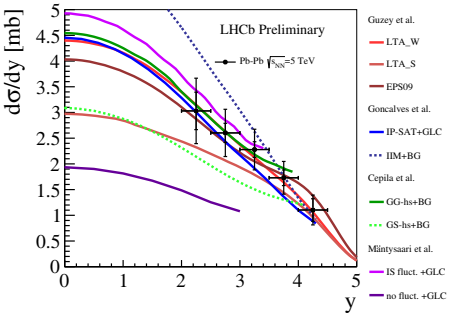

Fig. 2. Differential cross-section for coherent J/ψ production compared to different phenomenological predictions. The LHCb measurements are shown as points, where inner and outer error bars represent the statistical and the total uncertainties respectively.

[2] S. R. Klein, J. Nystrand, J. Seger, Y. Gorbunov, J. Butterworth, STARlight: A Monte Carlo simulation program for ultra-peripheral collisions of relativistic ions, Comput. Phys. Commun. 212 (2017) 258–268. arXiv:1607.03838, doi:10.1016/j.cpc.2016.10.016.

[3] A. Adeluyi, C. A. Bertulani, Constraining Gluon Shadowing Using Photoproduction in Ultraperipheral pA and AA Collisions, Phys. Rev. C85 (2012) 044904. arXiv:1201.0146, doi:10.1103/PhysRevC.85.044904.

[4] V. P. Gonçalves, M. V. T. Machado, Vector meson production in coherent hadronic interactions: an update on predictions for RHIC and LHC, Phys. Rev. C84 (2011) 011902. arXiv:1106.3036, doi:10.1103/PhysRevC.84.011902.

[5] A. Cisek, W. Schäfer, A. Szczurek, Exclusive coherent production of heavy vector mesons in nucleus-nucleus collisions at LHC, Phys. Rev. C86 (2012) 014905. arXiv:1204.5381, doi:10.1103/PhysRevC.86.014905.

[6] C. A. Bertulani, S. R. Klein, J. Nystrand, Physics of ultra-peripheral nuclear collisions, Ann. Rev. Nucl. Part. Sci. 55 (2005) 271–310. arXiv:nucl-ex/0502005, doi:10.1146/annurev.nucl.55.090704.151526.

[7] M. G. Ryskin, Diffractive J/ψ electroproduction in LLA QCD, Z. Phys. C57 (1993) 89–92. doi:10.1007/BF01555742.

[8] M. Tanabashi, et al., Review of particle physics, Phys. Rev. D98 (2018) 030001.

[9] R. Aaij, et al., Precision luminosity measurements at LHCb, JINST 9 (2014) P12005. arXiv:1410.0149, doi:10.1088/1748-0221/9/12/P12005.

[10] R. Aaij, et al., LHCb detector performance, Int. J. Mod. Phys. A30 (2015) 1530022. arXiv:1412.6352, doi:10.1142/S0217751X15300227.

[11] R. Aaij, et al., Central exclusive production of J/ψ and $\psi(2S)$ mesons in pp collisions at $\sqrt{s}$ = 13 TeVsubmitted to JHEP. arXiv:1806.04079.

[12] Study of coherent J/ψ production in lead-lead collisions at $\sqrt{s_{\rm NN}}$ = 5 TeV with the LHCb experiment, Tech. Rep. LHCb-CONF-2018-003. CERN-LHCb-CONF-2018-003, CERN, Geneva (May 2018).
URL `https://cds.cern.ch/record/2320135`

[13] V. P. Gonçalves, M. V. T. Machado, B. Moreira, F. S. Navarra, G. S. dos Santos, Color dipole predictions for the exclusive vector meson photoproduction in pp, pPb, and PbPb collisions at run 2 LHC energies, Phys. Rev. D96 (9) (2017) 094027. arXiv:1710.10070, doi:10.1103/PhysRevD.96.094027.

[14] J. Cepila, J. G. Contreras, M. Krelina, Coherent and incoherent J/ψ photonuclear production in an energy-dependent hot-spot model, Phys. Rev. C97 (2) (2018) 024901. arXiv:1711.01855, doi:10.1103/PhysRevC.97.024901.

[15] H. Mäntysaari, B. Schenke, Probing subnucleon scale fluctuations in ultraperipheral heavy ion collisions, Phys. Lett. B772 (2017) 832–838. arXiv:1703.09256, doi:10.1016/j.physletb.2017.07.063.